Reductive liquefaction of lignin to monocyclic hydrocarbons: ReS2/Al2O3 as efficient char inhibitor and hydrodeoxygenation catalyst

N.B. When citing this work, cite the original published paper.

(article starts on next page)

Reductive liquefaction of lignin to monocyclic hydrocarbons: ReS2/Al2O3 as efficient char inhibitor and hydrodeoxygenation catalyst

Pouya Sirous-Rezaei *, Derek Creaser , Louise Olsson

Competence Center for Catalysis, Department of Chemistry and Chemical Engineering, Chalmers University of Technology, SE-412 96 Gothenburg, Sweden

A R T I C L E   I N F O

A B S T R A C T

Thermochemical processing of lignin ends up with a major problem which is the high yield of char remained from lignin conversion, causing low yields of desired products. The ReS_2/Al_2O_3 catalyst, used in this work, exhibited a high char-suppressing potential and high hydrodeoxygenation efficiency in the reductive liquefaction of kraft lignin. Compared to $NiMo/Al_2O_3$, as a conventional sulfide catalyst, ReS_2/Al_2O_3 showed significantly better catalytic performance with 72.4 % lower char yield, due to its high efficiency in stabilizing the lignin-depolymerized fragments. The remarkable catalytic performance of ReS_2/Al_2O_3 is attributed to its high oxophilicity, the metal-like behavior of rhenium sulfide and sufficient acidity. The effects of reaction temperature and different catalyst supports (Al_2O_3, ZrO_2 and desilicated HY zeolite) were also studied. In an alkali (NaOH)-assisted depolymerization of lignin, it was revealed that ReS_2/Al_2O_3-to-NaOH (stabilization-to-depolymerization) ratio plays a crucial role in determining the reaction pathway toward either solid char residues or liquid monomeric products.

1. Introduction

Lignin, the most abundant renewable aromatic material on Earth, can be potentially exploited for the sustainable supply of fuels and chemicals which are currently derived from rapidly depleting and greenhouse gas emitting fossil resources [1–5]. Lignin, constituting 15–30 % of the biomass weight and up to 40 % of the biomass energy, is an amorphous and highly cross-linked macromolecule composed of the three primary phenylpropane monomers of *p*-coumaryl, coniferyl and sinapyl alcohols [6–10]. It can be processed via various depolymerization techniques for the production of high-value platform chemicals such as phenolics, aromatics and alkanes [11]. Today, industries such as pulp and paper manufacturing and lignocellulosics-to-ethanol processes produce large amounts of lignin as a by-product which is mostly burnt for use as an internal energy input [12–16]. Therefore, development of efficient processes for feasible utilization of lignin is highly important both in terms of environmental and economic aspects. In recent years, different thermochemical approaches (e.g., liquefaction and pyrolysis) have been applied for processing of lignin materials under reductive, neutral and oxidative atmospheres to produce value-added products (e. g., aromatic and cycloalkane hydrocarbons and phenolic compounds) [17,18]. However, there is a major problem in the processing of lignin,

which is the high formation of char solid residues remaining from the conversion of lignin, causing a low yield of desired target products [19–24]. This happens since lignin fragments from degradation of lignin polymer are highly reactive and undergo rapid repolymerization to form large amounts of char [25]. This necessitates the development of the catalytic systems which can effectively suppress char-forming condensation reactions.

In the reductive approaches, aiming to develop lignin-to-hydrocarbon processes, the most commonly tested catalysts can be divided into three groups: (i) transition (e.g., Ni, Cu)/noble (e.g., Pd, Pt, Ru) metal-based catalysts used in metallic form; (ii) metal oxide catalysts (e.g., MoO_x, ReO_x); (iii) conventional sulfide catalysts (e.g., $NiMo/Al_2O_3$, $CoMo/Al_2O_3$) currently being applied in refineries for hydrotreating purposes [19,26–36]. Meanwhile, different metal phosphide (e. g., MoP, Ni_2P), nitride (e.g., Mo_2N) and carbide (e.g., Mo_2C) catalysts have also been widely tested for the hydrodeoxygenation (HDO) of lignin model compounds [3]. The problem with the first two groups is that, although they mostly have high hydrogenation efficiency, their application is limited to sulfur-free lignin materials since they can be readily poisoned and deactivated in the presence of sulfur. The conventional sulfide catalysts have also been reported to give a high char yield from the conversion of lignin. Agarwal et al. [31] reported a char

---

* Corresponding author.
  E-mail address: pouya.rezaei@chalmers.se (P. Sirous-Rezaei).

yield of 23.3 wt% produced in the liquefaction of kraft pine lignin at 450 °C and 100 bar H_2 using CoMo/Al_2O_3 as a conventional hydrotreatment sulfide catalyst. In another work performed by the same group [32] for hydrotreatment of kraft lignin at 350 °C and 100 bar H_2, the solid residue yields of 20.5 and 35.4 wt% were obtained over conventional sulfide catalysts of NiMo/Al_2O_3 and CoMo/Al_2O_3, respectively. Considering that the majority of commercially available lignins have sulfur content (sulfite and kraft lignins with 3.5–8.0 % and 1.0–3.0 % sulfur, respectively), development of novel sulfur-resistant catalysts with high HDO efficiency can be an important strategy for the future supply of fuels and chemicals from lignin feedstocks [2,37]. Sulfur-resistant catalysts could also be applied for co-processing of lignin materials with other sulfur-containing feedstocks. This is particularly important for the feasibility of the integration of lignin processing with the existing petroleum refinery units with sulfur-containing input streams to improve the cost-effectiveness of lignin valorization.

To meet the above-mentioned challenges, and as a step towards an applicable and efficient lignin-to-hydrocarbon process, this work aimed to develop a catalyst with three major properties: (i) sulfur resistance; (ii) high char-suppressing potential; (iii) high HDO efficiency. In this study, rhenium sulfide was tested as a catalyst for HDO of *m*-cresol (as a model lignin-derived phenolic compound) and reductive liquefaction of kraft lignin, and its performance was compared with that of nickel-molybdenum sulfide which is a well-established conventional sulfide catalyst. To the best of our knowledge, this is the first use of rhenium sulfide for the conversion of a lignin feedstock. Rhenium sulfide has been reported in literature to be an active catalyst for hydro-desulfurization and hydrodenitrogenation reactions [38], and metallic rhenium is known as a catalyst with high hydrogenation efficiency [39]. Recently, hydrodeoxygenation of some phenolic compounds have also been performed using different rhenium phases (metal, oxide and sulfide) [40–42]. Moreover, rhenium has a considerably lower price compared to noble metals like Pd, Pt, Ru, Rh and Ir, and it also may have a lower price in the future with the enhanced demand for rhenium compounds and its increased commercial exploitation. Therefore, rhenium sulfide was selected to study its HDO activity and catalytic performance in the conversion of lignin. γ-Alumina, zirconia and desilicated HY zeolite were used as support materials for the rhenium sulfide catalysts in this work. An alkali-assisted depolymerization was also carried out to achieve an enhanced lignin depolymerization, and to study the correlation between depolymerization rate and stabilization rate as a key factor for suppressing char formation in a lignin liquefaction process.

2. Experimental

2.1. Catalyst preparation

NiMo/Al_2O_3, Re/Al_2O_3, Re/ZrO_2 and Re/HY were examined as catalysts in this work. HY, used as catalyst support, was a mesoporous zeolite obtained by desilication of a commercial Y zeolite (Zeolyst, CBV 780, SiO_2/Al_2O_3 molar ratio: 80) through alkaline treatment in a 0.3 M NaOH solution with mild stirring at 80 °C for 60 min. Then, the sample was filtered, washed with distilled water, and dried at 110 °C overnight. Subsequently, the desilicated zeolite was converted to the protonic form by three successive ion exchanges with a 1 M aqueous NH_4Cl solution at 80 °C for 4 h, followed by drying at 110 °C overnight and calcination at 550 °C for 12 h with a heating ramp of 2 °C min^{-1}. As a result of desilication, the SiO_2/Al_2O_3 molar ratio of HY zeolite was decreased from 80 to 36. Supported rhenium catalysts were obtained by incipient wetness impregnation of γ-Al_2O_3 (Puralox SCCa 150/200, Sasol), ZrO_2 (with monoclinic crystalline structure, SZ 31164, NORPRO) and HY with an aqueous solution of NH_4ReO_4 (Sigma-Aldrich). The NiMo/Al_2O_3 catalyst was prepared through incipient wetness co-impregnation of γ-Al_2O_3 with an aqueous solution containing both $(NH_4)_6Mo_7O_{24}·4H_2O$ and Ni$(NO_3)_2·6H_2O$ (Sigma-Aldrich). The amount of rhenium loaded on all the

supports was approximately 3 wt% (2.8, 2.8 and 2.7 wt% on Al_2O_3, ZrO_2 and HY supports, respectively), and the loading amounts of nickel and molybdenum metals on alumina support were 4.8 and 14.6 wt%, respectively (determined by quantitative XRF). At these metal loading amounts, both rhenium and nickel-molybdenum catalysts gave similar conversions for the HDO of *m*-cresol (based on initial experiments). Therefore, these metal loading amounts were selected to study the performance of the catalysts in the liquefaction of lignin. After impregnation, the catalysts were dried first at 60 °C (12 h) and then at 110 °C (12 h), with subsequent calcination at 550 °C for 12 h. Prior to reaction, the prepared catalyst was sulfided with dimethyl disulfide (DMDS, ≥ 99 %, Sigma-Aldrich) in the presence of 20 bar hydrogen (99.9 %, AGA) at 340 °C for 4 h in a Parr autoclave reactor.

2.2. Catalyst characterization

The crystalline structure of the catalysts was determined using X-ray diffraction (XRD) on a Bruker AXSD8 Advance X-ray powder diffractometer with Cu Kα radiation (λ = 1.542 Å). The chemical analysis of catalysts was carried out using an X-ray fluorescence (XRF) instrument (PANalytical Epsilon 3XL). The textural properties of the samples were determined by nitrogen isothermal (−196 °C) adsorption-desorption using a TriStar 3000 instrument. Transmission electron microscopy (TEM) images were acquired with a high angle annular dark field (HAADF) detector using a FEI Titan 80–300 operating at the accelerating voltage of 300 kV. The electronic states of the supported metals were determined by X-ray photoelectron spectroscopy (XPS) measurement using a PerkinElmer PHI 5000 VersaProbe III Scanning XPS Microprobe.

The acidity of the catalyst samples was measured by temperature programmed desorption of ammonia (NH_3-TPD) and ethylamine (ethylamine-TPD) using an experimental setup consisting of mass flow controllers (MFC, Bronkhorst) for gas mixing, a quartz tube containing the sample in a temperature-controlled furnace and a mass spectrometer (MS, Hiden HPR-20 QUI) for measuring the amount of ammonia or ethylene in the outlet stream. Before ammonia or ethylamine adsorption, the presulfided catalyst was pretreated in Argon at 100 °C for 30 min. Then, it was exposed to 1555 ppm of NH_3 or 543 ppm of ethylamine at 100 °C for 2 h. Afterwards, the sample was flushed with argon for 30 min to eliminate physisorbed ammonia/ethylamine. The desorption measurement was performed by heating the sample to 800 °C with a ramp of 10 °C min^{-1} under an argon flow (20 ml min^{-1}). Thermogravimetric analysis (TGA) of the samples showed that no thermal decomposition occurs up to 800 °C (shown in Fig. S1, Supplementary Information). The samples were heated from 35 to 800 °C with a heating ramp of 10 °C min^{-1} in a stream of nitrogen gas (30 ml min^{-1}).

2.3. Catalytic activity measurement

The hydrodeoxygenation (HDO) of *m*-cresol (≥ 99 %, Sigma-Aldrich) and reductive liquefaction of kraft lignin (product number: 370959, Sigma-Aldrich) (with 2.1 wt% sulfur content measured by ICP-AES and ICP-SMS) were conducted in a 300 ml Parr autoclave reactor. The elemental and proximate compositions of the kraft lignin sample are presented in Table S1, Supplementary Information. In each experiment, 3 g reactant, 90 ml hexadecane solvent (≥ 99 %, Sigma-Aldrich) and a certain amount of presulfided catalyst were added to the reactor. The lowest catalyst-to-feed ratio applied in this work was 1:3 (at least 1 g solid catalyst) in order to minimize mass transfer limitations for a better comparison of the catalytic performance of the different catalysts. The loaded reactor was sealed, and the air inside it was evacuated by pressurizing/depressurizing the reactor three times with first nitrogen and then hydrogen gas. Afterward, the reactor was pressurized with 30 bar of hydrogen gas and then heated up to the reaction temperature (340 or 400 °C). The reactor pressure was 56–57 and 65–68 bar at the reaction temperatures of 340 and 400 °C, respectively. The reactions were carried out with a stirring rate of 1000 rpm for a duration of 3 h for HDO of

m-cresol and 6 h for lignin conversion. In the experiments for HDO of *m*-cresol, 88 mg DMDS was added to maintain the sulfidation of catalysts during the reaction, and in some experiments for lignin conversion, NaOH (≥ 98 %, Sigma-Aldrich) was added for enhanced depolymerization of lignin via alkali-catalyzed degradation. The liquid composition in HDO of *m*-cresol was monitored by collecting samples at intervals of 30 min. When the reaction was complete, the reactor was immediately quenched to room temperature and the solid phase was separated from the liquid product by vacuum filtration. The solid residue remaining from lignin conversion reactions was washed with acetone to remove the organics and solvent absorbed on the solid particles. After acetone extraction, the solid fraction (catalyst, char residues and unconverted lignin) was dried at 110 °C and weighed. Subsequently, the solid fraction was washed with dimethyl sulfoxide (DMSO, ≥ 99.9 %, Sigma-Aldrich) to dissolve and remove unconverted lignin. Then, the solids were washed with acetone to remove DMSO and dried at 110 °C overnight. The difference in the weight of solids before and after DMSO extraction was assigned to the amount of unconverted lignin which was almost negligible (below 2 wt% on feed) in all the experiments. The liquid phase products were analyzed by a two-dimensional gas chromatography system (GC × GC, Agilent 7890−5977A). The products were separated by two columns with different polarity (a DB-5 ms column (30 m × 0.25 mm × 0.25 mm) for the first dimension and a BPX-50 column (2.5 m × 0.10 mm × 0.10 mm) for the second dimension), and detected by mass spectrometer (MSD) and flame ionization (FID) detectors for qualitative and quantitative analysis, respectively. The product yields were measured by an external standard calibration method, with calibration curves using several known concentrations (mass) that were related to the FID peak areas (with $R^2 > 0.99$). This calibration was conducted for a number of individual compounds such as toluene, ethylbenzene, propylbenzene, methylcyclohexane, cyclohexane, guaiacol, *m*-cresol, phenol, propylphenol, naphthalene, methylnaphthalene, tetralin, dimethyltetralin, methylbiphenyl, benzyl phenyl ether, biphenol and phenanthrene. Experiments were repeated 2–3 times to ensure the reproducibility of the data.

3. Results and discussion

3.1. Catalytic performance of sulfided Re/Al₂O₃ and NiMo/Al₂O₃

3.1.1. HDO of m-cresol: Re/Al₂O₃ vs. NiMo/Al₂O₃

Fig. 1 presents *m*-cresol conversion levels and product selectivities with time over sulfided Re/Al₂O₃ and NiMo/Al₂O₃ catalysts at 340 °C. Both catalysts exhibited a similar trend for the conversion of *m*-cresol, giving a complete conversion after 2.5 h reaction. Considering that the number of rhenium atoms loaded on alumina support is almost ten times less than that of molybdenum atoms (the loading amounts of Re and Mo were approximately 3 and 15 wt%, respectively), it could be inferred that rhenium sulfide is more active than molybdenum sulfide as a hydrogenation promoter. After 3 h reaction, the mass yields of methylcyclohexane, methylcyclohexene, ethylcyclopentane and toluene were 63.9, 0.0, 6.2 and 10.9 wt% over NiMo/Al₂O₃, and 75.1, 0.6, 8.2 and 5.2 wt% over Re/Al₂O₃, respectively (shown in Fig. 2).

As can be seen from the products obtained by the conversion of *m*-
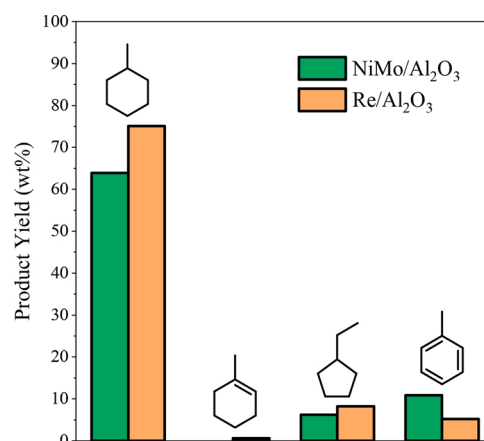
Fig. 2. Product yields (wt% on feed) obtained by the HDO of *m*-cresol over Re/Al₂O₃ and NiMo/Al₂O₃. Reaction conditions: catalyst, 1 g; *m*-cresol, 3 g; hexadecane, 90 ml; reaction temperature, 340 °C; H₂ initial pressure, 30 bar; reaction time, 3 h.

Fig. 1. Conversion and product distribution for the HDO of *m*-cresol over Re/Al₂O₃ and NiMo/Al₂O₃ at different reaction times. Reaction conditions: catalyst, 1 g; *m*-cresol, 3 g; hexadecane, 90 ml; reaction temperature, 340 °C; H₂ initial pressure, 30 bar.

cresol, the HDO reaction proceeds through both ring hydrogenation (HYD) and direct deoxygenation (DDO) pathways over both NiMo/Al$_2$O$_3$ and Re/Al$_2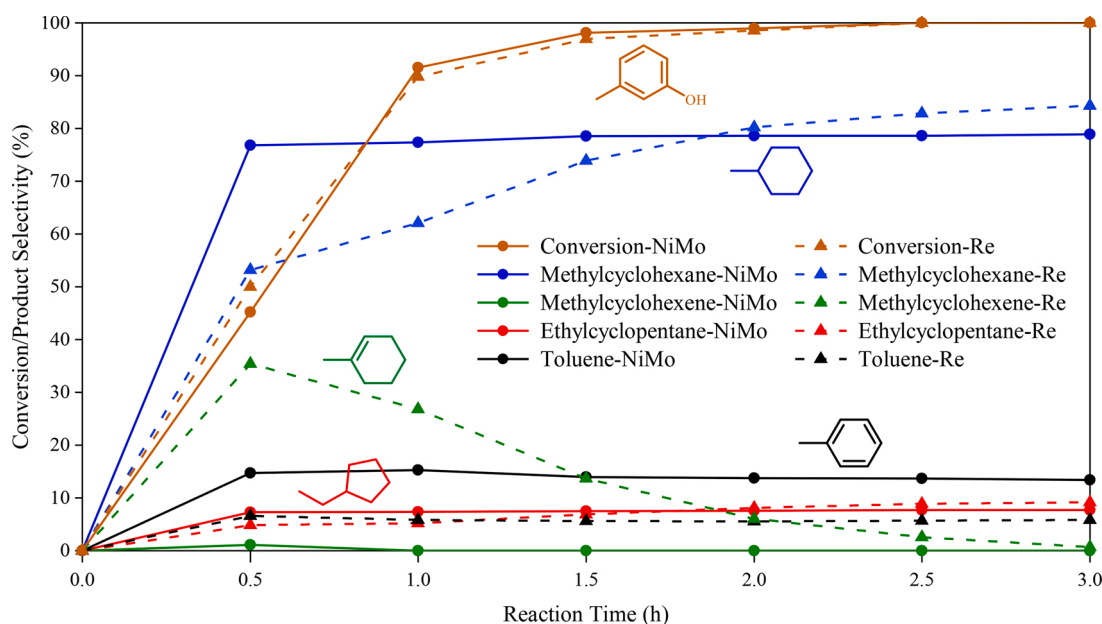O_3$ catalysts. In the DDO mechanism, *m*-cresol is adsorbed through its oxygen atom on the catalyst active site which is a sulfur vacancy, and the double bond on the phenolic ring close to the C$_{aromatic}$-OH bond is hydrogenated to a single bond. This results in a temporary removal of the electron delocalization effect of the out-of-plane lone pair electron orbital of oxygen onto the phenolic ring π bond orbital and, in turn, a weaker C—O bond which can be easily cleaved by dehydration over an adjacent acid site, giving toluene as the final aromatic hydrocarbon product [43–45]. In the ring hydrogenation pathway, the co-planar adsorption of *m*-cresol on the catalyst surface leads to ring saturation, producing methylcyclohexanol as an intermediate. This is then followed by dehydration to form methylcyclohexene which undergoes subsequent hydrogenation to be converted into methylcyclohexane as the saturated cyclic hydrocarbon product [43, 46]. Ring hydrogenation was the dominant HDO pathway over both catalysts, giving high methylcyclohexane-to-toluene molar ratios of 5.5 and 13.6 over NiMo/Al$_2$O$_3$ and Re/Al$_2$O$_3$, respectively. The higher methylcyclohexane-to-toluene ratio over Re/Al$_2$O$_3$ indicates higher hydrogenation activity of this catalyst. In a study for hydrodeoxygenation of 2-ethylphenol over sulfided Mo-based catalysts, it was suggested that ring hydrogenation via co-planar adsorption requires two neighboring sulfur vacancies as active site, while DDO mechanism occurs on a single sulfur vacancy [47]. It is also inferred from the product selectivities over time that toluene, produced via DDO mechanism, does not undergo ring hydrogenation and remains unchanged by the end of the reaction. Another difference between the two examined catalysts is the rate of the hydrogenation of methylcyclohexene which is lower over Re/Al$_2$O$_3$. Methylcyclohexene was almost undetectable during the reaction using NiMo/Al$_2$O$_3$, indicating that this intermediate only exists for a short time before it is rapidly hydrogenated to methylcyclohexane. In contrast, methylcyclohexene was observed in relatively high quantities in the first 2 h of the reaction over Re/Al$_2$O$_3$. This might be ascribed to the slower adsorption of this intermediate on hydrogenation active sites on the surface of Re/Al$_2$O$_3$, more likely due to the higher number of phenolic rings hydrogenated over this catalyst. Ethylcyclopentane was also produced in low yield over both catalysts via acid-catalyzed ring contraction of methylcyclohexane [48].

3.1.2. Lignin conversion: Re/Al$_2$O$_3$ vs. NiMo/Al$_2$O$_3$

The yields of monocyclic products and char residues obtained by the conversion of kraft lignin over different catalysts are shown in Table 1. Lignin was almost fully converted (> 98 %) in all the experiments, and other products (not shown in Table 1) are mainly heavy oligomers (non-detectable by GC), tetralins, indenes, naphthalenes, water and gas products. A comparison of the monocyclic product yields of Re/Al$_2$O$_3$ and NiMo/Al$_2$O$_3$ at the reaction temperature of 340 °C (entries 2 and 3,

Table 1) reveals a remarkable superiority of rhenium sulfide catalyst; the total monocyclic product yields achieved over Re/Al$_2$O$_3$ and NiMo/Al$_2$O$_3$ were 21.5 and 4.6 wt%, respectively. This is mainly due to the different amounts of char remaining from the conversion of lignin over these two catalysts, with the yields of 40.6 wt% over NiMo/Al$_2$O$_3$ and 11.2 wt% over Re/Al$_2$O$_3$ (the images of char residues remaining from lignin conversion are shown in Fig. S2, Supplementary Information). This significant difference clearly illustrates the high catalytic efficiency of Re/Al$_2$O$_3$ for suppressing char formation which is a major problem in thermochemical processes for conversion of lignin. The typical high char yields from lignin conversion is a result of the low stability and high reactivity of lignin-derived intermediates which undergo condensation reactions to form heavy compounds as solid char residues [49]. Radical coupling, quinone methide and vinyl condensation are some significant condensation mechanisms which lead to high amounts of char remaining from lignin conversion [25]. Low char yield obtained over alumina-supported rhenium sulfide reveals that this catalyst is highly effective for stabilizing the lignin-derived reactive compounds and, in turn, suppressing condensation reactions. This could be due to higher activity of the rhenium sulfide catalyst for hydrogenating free radicals and preventing radical coupling in a reducing atmosphere. The char-suppressing effect of hydrogenation could also be observed by a comparison of the char yield of the alumina-supported hydrogenation promoters (rhenium and nickel-molybdenum sulfides) with that of the pure alumina support. As shown in Table 1, entries 1–3, the highest char yield (48.2 wt%) was obtained using the pure alumina support, indicating a higher condensation rate in the absence of hydrogenation active sites. Meanwhile, almost no monocyclic hydrocarbons were produced over Al$_2$O$_3$ due to the absence of hydrogenation activity.

The high efficiency of the rhenium sulfide catalyst should be recognized in light of the fact that the low char yield of 11.2 wt% was obtained in this case using hexadecane as solvent, which is not a good solubilizer of lignin-derived components. Therefore, rhenium sulfide could be effectively used in the absence of the oxygen-containing polar solvents (e.g., alcohols) which are typically used for lignin liquefaction due to their higher solubility for lignin fragments. This makes rhenium sulfide a potential catalyst to be used for co-processing of lignin with hydrocarbon feedstocks in conventional petroleum refinery units. Moreover, considering the resistance of this metal sulfide catalyst to sulfur poisoning, it can be effectively used in hydrotreating of sulfur-containing lignin feedstocks. In addition, although rhenium is more expensive than molybdenum, but it has a lower price compared to the other noble metals with high hydrogenation activity (e.g., Pt, Ru, Ir and Rh). It could also be noticed that the low loading of rhenium on the catalyst support (like 3 wt% in this work compared to the typically high loading amounts of molybdenum (12–15 wt%) in commercial molybdenum-based catalysts) can increase the cost-effectiveness of rhenium-based catalysts. They could also be more economically

Table 1

Yields of monocyclic products and char (wt% on feed) obtained by the catalytic liquefaction of kraft lignin over different catalysts. Reaction conditions: lignin, 3 g; hexadecane, 90 ml; H$_2$ initial pressure, 30 bar; reaction time, 6 h.

Entry	Catalyst	T (°C)	Monocyclic product yield (wt%)				Char yield (wt%)
			Cycloalkanes	Arenes	Phenolics	Total	
1	Al$_2$O$_3$ (1 g)	340	0.0	0.2	3.1	3.3	48.2
2	NiMo/Al$_2$O$_3$ (1 g)	340	3.1	1.5	0.0	4.6	40.6
3	Re/Al$_2$O$_3$ (1 g)	340	4.2	3.1	14.2	21.5	11.2
4	Re/Al$_2$O$_3$ (1 g)	400	8.3	8.5	0.7	17.5	8.5
5	Re/ZrO$_2$ (1 g)	400	6.2	5.0	10.6	21.8	10.7
6	Re/HY (1 g)	400	4.6	3.9	14.9	23.4	11.8
7	Re/Al$_2$O$_3$ (1 g) + HY (1 g)	400	4.7	6.8	2.3	13.8	15.0
8	Re/Al$_2$O$_3$ (1 g) + NaOH (1 g)	400	6.0	5.9	4.4	16.3	44.3
9	Re/Al$_2$O$_3$ (2 g) + NaOH (1 g)	400	12.3	8.6	0.0	20.9	23.1
10	Re/Al$_2$O$_3$ (2 g) + NaOH (0.5 g)	400	13.5	11.1	0.0	24.6	11.3
11	NaOH (1 g)	400	0.0	0.0	4.2	4.2	47.0
12	Re/Al$_2$O$_3$ (2 g)	400	10.5	8.1	0.0	18.6	5.4

attractive in the future with the increased commercial exploitation of rhenium due to enhanced demand for rhenium compounds.

3.1.3. Catalytic characteristics of rhenium sulfide as HDO catalyst

One characteristic of rhenium which makes it a highly active metal for catalyzing deoxygenation reactions is its high oxophilicity [39]. The oxophilic rhenium species are well known to be efficient for activation of oxy-compounds by strong adsorption of oxygen-containing functional groups to the surface of catalyst. Hence, this facilitated adsorption and strengthened interaction could be a reason for the effective performance of rhenium sulfide for lignin degradation (through cleavage of ether linkages) and HDO of lignin-derived phenolic compounds.

The high catalytic activity of rhenium sulfide can also be correlated to the low binding energy shift between the rhenium sulfide phase and rhenium metal. As depicted by XPS analysis, presented in Fig. 3 and Table 2, the binding energies of the Re $4f_{7/2}$ component of the 4f doublet for the ReO_x/Al_2O_3 catalyst are 44.03 and 46.15 eV which are assigned to Re^{6+} (ReO_3) and Re^{7+} (Re_2O_7), respectively [50,51]. After sulfidation, this catalyst displayed two Re $4f_{7/2}$ contributions with binding energies of 41.36 and 42.57 eV which are attributed to ReS_2 species and some oxysulfide species (S-Re-O), respectively [52,53]. As the relative proportion values show, rhenium sulfide on alumina support exists mainly (87 %) as ReS_2 with the binding energy close to that of rhenium metal (40.4–40.7 eV) [54,55]. The low binding energy difference between the rhenium sulfide phase and rhenium metal indicates that a high degree of the characteristic of metal is preserved during sulfidation,

Table 2
NH$_3$-TPD and XPS data.

Catalyst	Acidity[a] (mmol g^{-1})				XPS binding energy and surface atomic ratio		
	Total	Weak	Medium	Strong	Re $4f_{7/2}$ (eV)	Re $4f_{7/2}$ (eV)	S/Re
Al$_2$O$_3$	0.364	0.124 (34 %)	0.145 (40 %)	0.095 (26 %)			
ReO$_x$/Al$_2$O$_3$					44.03 (35 %)	46.15 (65 %)	
ReS$_x$/Al$_2$O$_3$	0.451	0.129 (29 %)	0.204 (45 %)	0.118 (26 %)	41.36 (87 %)	42.57 (13 %)	2.2
ReS$_x$/ZrO$_2$	0.236	0.083 (35 %)	0.106 (45 %)	0.047 (20 %)	41.94 (84 %)	43.16 (16 %)	3.1
ReS$_x$/HY	0.214	0.052 (24 %)	0.094 (44 %)	0.068 (32 %)	41.62 (75 %)	42.53 (25 %)	2.4

[a] Acid site strength was determined by ammonia desorption measurements at different temperature ranges: weak, < 300 °C; medium, 300−600 °C; strong, > 600 °C.

giving a metal-like nature to the metal-sulfur valence molecular orbitals. As metallic rhenium is believed to be highly effective for activation of H$_2$ molecules [39], this metal-like character of rhenium sulfide species leads to a facilitated uptake of hydrogen and a high rate of the dissociation of molecular H$_2$, giving an enhanced hydrogenation efficiency. The low char yields obtained from the liquefaction of lignin in the presence of rhenium-based catalyst could be associated to the high
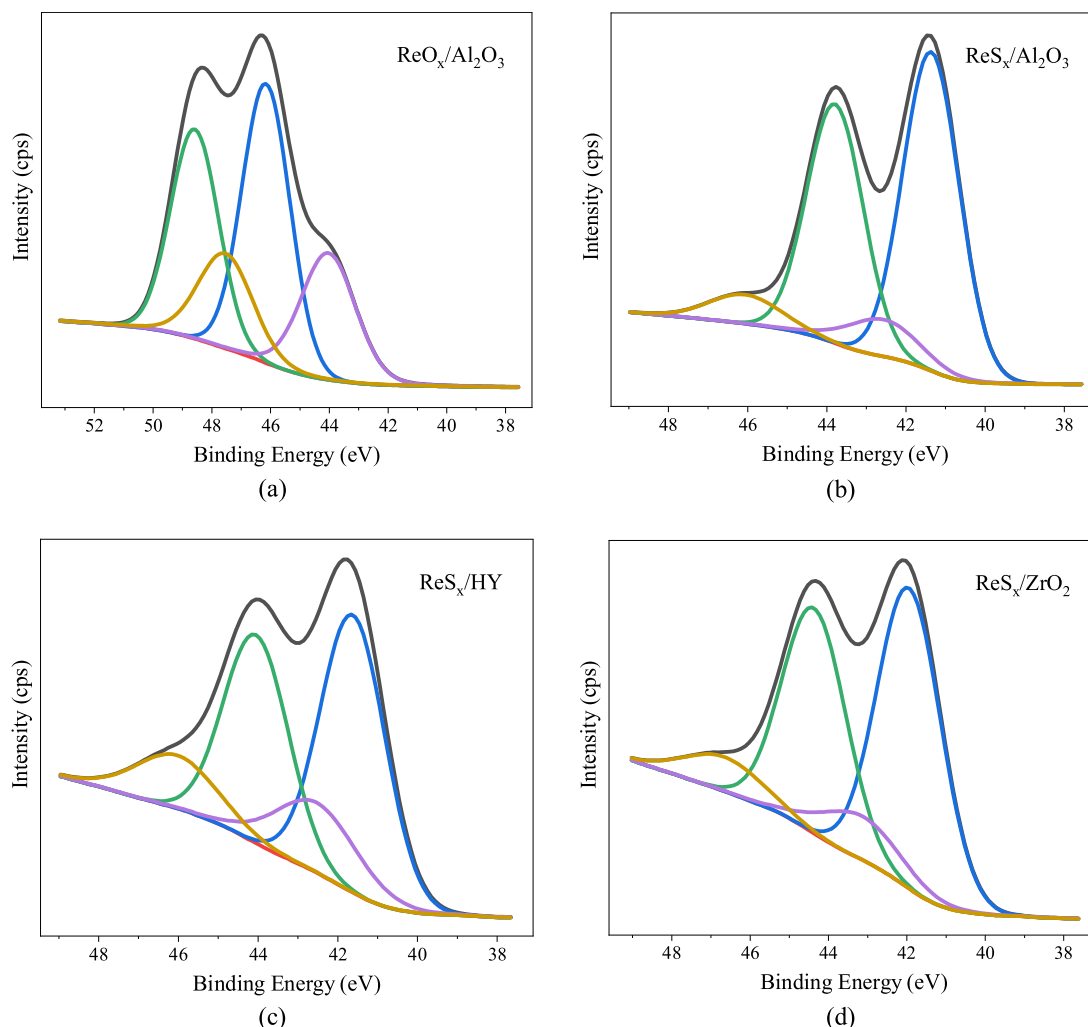

Fig. 3. XPS spectra for Re 4f region of (a) ReO$_x$/Al$_2$O$_3$, (b) ReS$_x$/Al$_2$O$_3$, (c) ReS$_x$/HY and (d) ReS$_x$/ZrO$_2$ catalysts.

hydrogenation efficiency of rhenium sulfide; the highly reactive lignin derivatives can be stabilized via rapid hydrogenation, and thus, undesired coupling reactions and repolymerization to char residues can be effectively inhibited. The XPS analysis of the spent alumina-supported rhenium sulfide catalyst used for the HDO of *m*-cresol shows that the sulfide state of rhenium was maintained during the HDO reaction (presented in Fig. S3). The binding energy of ReS_2 species on the spent catalyst was similar to that of the fresh catalyst, while the Re $4f_{7/2}$ contribution attributed to oxysulfide species disappeared, indicating the complete sulfidation of these species during the HDO reaction.

Rhenium-induced acidity can also play an important role in catalytic performance of rhenium species by improving acid-catalyzed reactions. As revealed by NH_3-TPD data presented in Fig. 4 and Table 2, the catalyst acidity was increased by the addition of rhenium species; the total acidity of Al_2O_3 and ReS_2/Al_2O_3 are 0.364 and 0.451 mmol g^{-1}, respectively. The amount of acidity induced by rhenium sulfide species should be higher than the difference in acid amounts of Al_2O_3 and ReS_2/Al_2O_3, since the impregnated metal species cover a portion of the acid sites of the support, and the amount of ammonia desorption (in TPD analysis) from support in ReS_2/Al_2O_3 is less than that from alumina support alone. It is also noticeable that, based on the acid strength distribution of these two catalysts, rhenium-induced acidity is mostly of medium strength; the densities of weak, medium and strong acid sites are 0.124, 0.145 and 0.095 mmol g^{-1} in Al_2O_3, and 0.129, 0.204 and 0.118 mmol g^{-1} in ReS_2/Al_2O_3, respectively. This increased acidity can particularly improve the cleavage of ether linkages of lignin, causing an enhanced rate of depolymerization [56]. As a result, lignin fragments can be converted into monomeric compounds before they undergo repolymerization to form heavy solid residues. Moreover, the acidity provided by rhenium species can also improve the dehydration step of HDO reaction, leading to an enhanced deoxygenation and increased hydrocarbon yield [45,57]. According to ethylamine-TPD analysis, the rhenium-induced acidity is mainly Lewis acidity. In ethylamine-TPD, ethylamine is adsorbed on Brønsted acid sites, and the ethyl-ammonium ions (formed via proton transfer) undergo the Hofmann elimination reaction to produce ethylene and ammonia at higher temperatures [58,59]. Therefore, the ethylene detected during ethylamine-TPD is quantified to measure Brønsted acidity. Based on the ethylene desorption profile (shown in Fig. S4), the density of Brønsted acid sites of ReS_2/Al_2O_3 is 0.022 mmol g^{-1} which constitutes 5% of the total acidity (0.451 mmol g^{-1}, measured by NH_3-TPD) of this catalyst, indicating that the catalyst acidity is mainly Lewis type.

3.2. Temperature-dependency of lignin conversion

The reaction pathway and product distribution in a lignin liquefaction process is a strong function of reaction temperature mainly due to the temperature dependence resulting from varying activation energies for the different series and parallel reactions taking place during lignin conversion. The significance of reaction temperature is more realized when it is considered that it greatly affects the rate of repolymerization reactions of lignin derivatives which lead to undesired formation of solid char residues. At low reaction temperatures (usually below 300 °C), low lignin depolymerization occurs due to low thermal cracking and inefficient catalytic degradation (e.g., hydrogenolysis), and instead, the repolymerization of highly reactive lignin-derived compounds yields a high char formation since these compounds cannot be catalytically stabilized at low temperatures [22]. Similarly, at high reaction temperatures (usually above 400 °C), significant char-forming reactions happen as a result of severe carbonization [21,22]. Therefore, the applied reaction temperature should be high enough to provide the activation energies required for both depolymerization of lignin and stabilization of reactive lignin derivatives (via e.g. hydrogenation and alkylation) on one hand, and not too high in order to cause carbonization reactions on the other hand. As mentioned before, Al_2O_3-supported rhenium sulfide could efficiently suppress char-forming reactions at 340 °C. In order to examine the stabilizing efficiency of this catalyst at an elevated temperature, the reaction temperature was increased to 400 °C while keeping other parameters constant. This caused a reduction in char yield from 11.2 to 8.5 wt% (entries 3 and 4, Table 1), indicating that Re/Al_2O_3 catalyst could more effectively stabilize lignin fragments at the higher temperature of 400 °C through an enhanced hydrogenation of free radicals. Importantly, this temperature increase caused a remarkably improved deoxygenation efficiency more likely due to the enhanced dehydration activity of the Re/Al_2O_3 catalyst at elevated temperature; the monocyclic hydrocarbon yield was increased from 7.3 to 16.8 wt%, and the monocyclic phenolic yield was decreased from 14.2 to 0.7 wt% by an increase of temperature from 340 to 400 °C (entries 3 and 4, Table 1). Consequently, the enhanced oxygen removal at 400 °C resulted in a lower monocyclic product yield of 17.5 wt% which was slightly higher (21.5 wt%) at 340 °C. Moreover, HDO reaction selectivity was also affected by the increase of temperature, and the higher temperature of 400 °C favored direct deoxygenation over ring hydrogenation; the monocyclic aromatic hydrocarbon selectivity was increased from 38.7 to 48.3 mol% by increasing temperature from 340 to 400 °C (shown in Fig. 5). This could be caused by the decreased
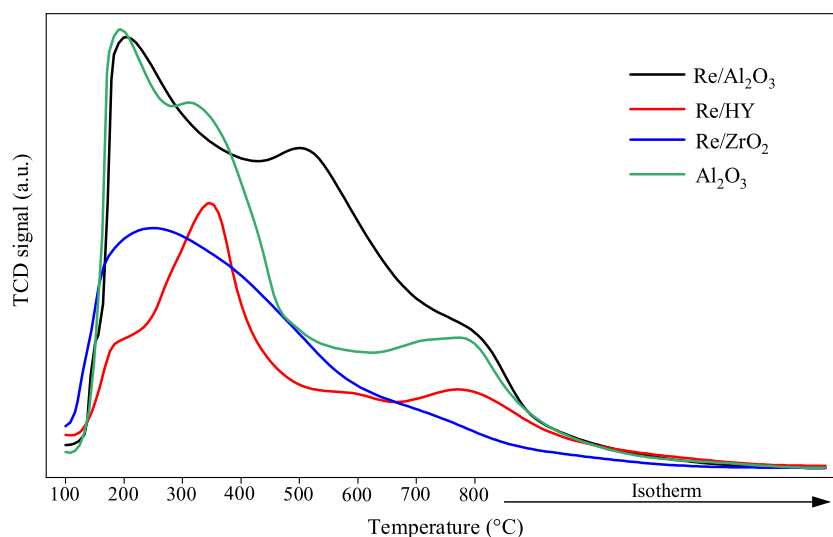

Fig. 4. NH_3-TPD profiles of catalysts (before TPD analysis, supported rhenium catalysts were sulfided in the presence of hydrogen with dimethyl disulfide at 340 °C for 4 h).
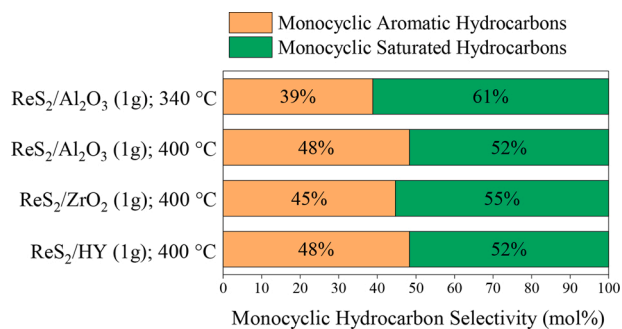
Fig. 5. Monocyclic hydrocarbon selectivity (mol%) obtained by the catalytic liquefaction of kraft lignin. Reaction conditions: lignin, 3 g; hexadecane, 90 ml; H_2 initial pressure, 30 bar; reaction time, 6 h.

availability of hydrogen on the surface of the catalyst at elevated temperature as a result of the reduced hydrogen adsorption due to its exothermic nature [60]. Lower hydrogen availability is favorable for the

DDO mechanism which requires less hydrogen consumption compared to the HYD reaction route. This is consistent with several previous studies reporting that HYD and DDO are the dominant reaction pathways taking place at low and high temperatures, respectively [61,62].

3.3. Effect of catalyst support: performance of Al_2O_3, ZrO_2 and HY zeolite

As can be seen from the yields and selectivities of monocyclic products obtained over Re/Al_2O_3, Re/ZrO_2 and Re/HY, presented in Table 1 (entries 4–6), catalyst support has a significant effect on catalytic performance and reaction pathway. For a better comparison of the catalytic activities of the supports, HY zeolite was desilicated to generate a mesoporous zeolitic structure with lower diffusion limitations of lignin fragments. The textural properties of the supports are shown in Table S2. HDO activity was remarkably affected by the choice of catalyst support, and monocyclic hydrocarbon yield was reduced in the order: Re/Al_2O_3 > Re/ZrO_2 > Re/HY. The monocyclic hydrocarbon yields were 16.8, 11.2 and 8.5 wt%, and monocyclic phenolic yields were 0.7, 10.6 and
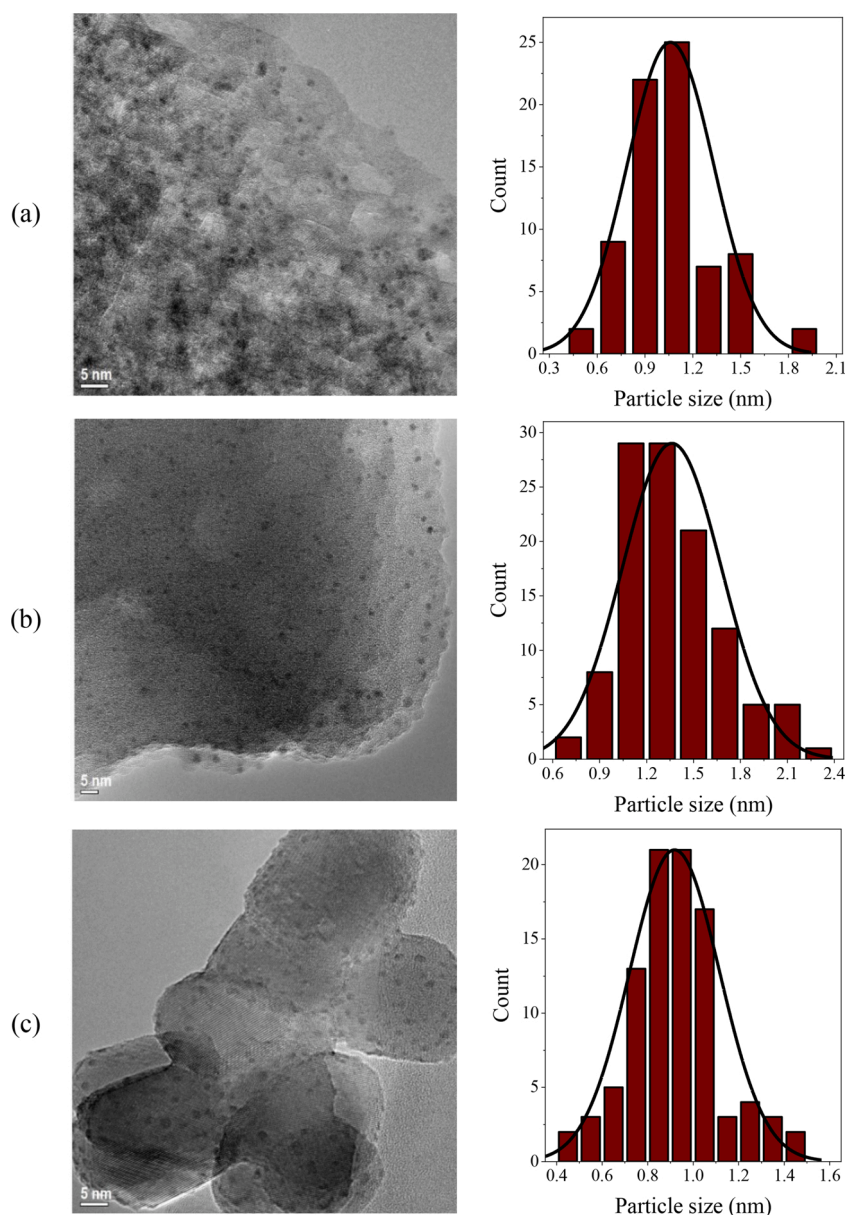

Fig. 6. TEM images and particle size distribution of (a) ReS_2/Al_2O_3, (b) ReS_2/HY and (c) ReS_2/ZrO_2 catalysts.

14.9 wt% over Re/Al$_2$O$_3$, Re/ZrO$_2$ and Re/HY catalysts, respectively, indicating that the use of alumina as catalyst support led to the highest deoxygenation efficiency. As a result of the enhanced oxygen removal over Re/Al$_2$O$_3$, this catalyst gave a lower mass yield of total monocyclic compounds compared to Re/ZrO$_2$ and Re/HY catalysts. It can be seen from the data shown in Fig. 5 that HDO reaction selectivity was not largely influenced by catalyst support, and the monocyclic aromatic hydrocarbon selectivity was similar (44.7–48.3 mol%) over Al$_2$O$_3$-, ZrO$_2$- and HY-supported rhenium catalysts. Similar to the HDO activity trend of the catalysts, the stabilizing efficiency was also decreased in the order: Re/Al$_2$O$_3$ > Re/ZrO$_2$ > Re/HY, giving the char yields of 8.5, 10.7 and 11.8 wt%, respectively.

To study the effect of the addition of a zeolitic catalyst to Re/Al$_2$O$_3$, a combination of Re/Al$_2$O$_3$ (1 g) and HY (1 g) was used as the catalytic system for the conversion of kraft lignin at 400 °C. The addition of zeolite had a negative effect and resulted in a reduction of monocyclic product yield from 17.5 to 13.8 wt% (entries 4 and 7, Table 1). This could be due to the condensation of lignin-derived fragments catalyzed by zeolite acid sites in the absence of a hydrogenation promoter, converting both hydrocarbons and oxygenates into catalytic coke deposited inside the zeolite channels [63].

TEM images, shown in Fig. 6, illustrate that rhenium species are well dispersed on all the supports as spherical particles. This is in agreement with previous studies reporting a high dispersion of rhenium particles on different catalyst supports [38,45,64]. The spherical structure of rhenium sulfide species on a γ-alumina support was also observed in a study by Quartararo et al. [65]. However, Escalona et al. [38] reported the presence of rhenium sulfide as both layered crystallites and spherical particles (with different ratios) on a γ-alumina support, suggesting that the ratio between the two structures depends on the sulfiding condition. The same group later showed that ReS$_2$ species supported on different materials had layered structure which was transformed to spherical structure (with lower S/Re ratio) when exposed to the electron beam for 15 min, as a result of the desulfurization to metallic Re under the beam [52]. However, this structural change under electron beam was not observed in our work, and the rhenium sulfide species appeared as spherical particles from the beginning of the exposure to the beam. The histograms of size distribution, presented in Fig. 6, indicate that the mean particle diameter of rhenium sulfide species is 1.1, 1.4 and 0.9 nm on Al$_2$O$_3$, HY and ZrO$_2$ supports, respectively. Besides, the two main lattice fringes in the TEM image of ReS$_2$/Al$_2$O$_3$ have interplanar spacings of about 0.20 and 0.14 nm, which correspond to the (400) and (440) reflections of the γ-alumina phase, respectively (shown in Figs. S5 and S6a). The difference in the catalytic performance of the supports could be correlated with their different acidic properties measured by NH$_3$-TPD analysis. The data presented in Table 2 and Fig. 4 illustrate that the acid site density of the catalysts decreased in the order: Re/Al$_2$O$_3$ (0.451 mmol g^{-1}) > Re/ZrO$_2$ (0.236 mmol g^{-1}) > Re/ HY (0.214 mmol g^{-1}). The higher acidity of Re/Al$_2$O$_3$ promotes the dehydration step of the HDO reaction to remove the oxygen atom of lignin-derived phenolics as water. Hence, it is supposed that the promoted dehydration, which is an acid-catalyzed reaction, leads to the high hydrocarbon yield achieved over the Re/Al$_2$O$_3$ catalyst. Moreover, as revealed by XPS data, shown in Fig. 3 and Table 2, catalyst support also affects the chemical state of the supported rhenium sulfide species, which this, in turn, can influence the reaction rate and pathway. The binding energy of ReS$_2$ species loaded on different supports decreased in the order: ReS$_2$/ZrO$_2$ (41.94 eV) > ReS$_2$/HY (41.62 eV) > ReS$_2$/Al$_2$O$_3$ (41.36 eV). Therefore, rhenium sulfide loaded on alumina support has the minimum binding energy difference with that of metallic rhenium, and in turn, exhibits the most metal-like behavior. Besides, based on the relative proportion values of Re 4f$_{7/2}$ components, the alumina support leads to the highest degree of sulfidation of rhenium oxide species (87 %) followed by zirconia (84 %) and HY zeolite (75 %) supports. Furthermore, the atomic ratios of S/Re on the different supports reduced in the order: ReS$_2$/ZrO$_2$ (3.1) > ReS$_2$/HY (2.4) > ReS$_2$/Al$_2$O$_3$ (2.2),

indicating that rhenium loaded on alumina support has the minimum attached sulfur ligands, resulting in the most sulfur-deficient sulfide phase and, in turn, the highest number of sulfur vacancies which can contribute to hydrogenation/hydrogenolysis reactions.

3.4. Alkali-assisted degradation of lignin: towards either desired monomers or undesired char

Base-catalyzed cleavage of lignin linkages, particularly aryl-alkyl ether bonds, is a well-studied approach for lignin depolymerization. A wide variety of low-cost and commercially available catalytic reagents such as NaOH, LiOH and KOH have been applied for alkaline degradation of lignin [3]. As an example for the mechanism of base-catalyzed degradation of lignin, the cleavage of β-O-4 linkages, as the most dominant aryl-alkyl ether bonds in lignin structure, occurs by the polarization promoted by a base catalyst [66,67]. Using NaOH as base catalyst, it is proposed that the sodium cation polarizes the β-O-4 ether linkage via formation of a cation adduct with lignin. As a result, the oxygen atom of the ether bond gains an increased negative partial charge, and in turn, less energy is required for heterolytic cleavage of this bond. This leads to the formation of a sodium phenolate along with a carbenium ion transition state which is subsequently neutralized by the hydroxide ion.

In this study, NaOH was added to the reaction system for an increased depolymerization degree and a higher yield of monomeric products. However, the ratio of the amount of Re/Al$_2$O$_3$ to the amount of added NaOH was critical for the fate of the converted lignin as either the desired target monomeric products or undesired solid char residues. The effect of this ratio is shown in Table 1 (entries 8–10). The addition of 1 g NaOH resulted in a large amount of char formation from lignin conversion (44.3 wt%), giving a monocyclic product yield of 16.3 wt% and monocyclic hydrocarbon yield of 11.9 wt% which were less than those obtained in the absence of NaOH (17.5 and 16.8 wt%, respectively). This is due to the high amount of additional NaOH which resulted in a high rate of base-catalyzed degradation and, in turn, a large number of lignin fragments produced in a short period of time at the beginning of the reaction. The amount of Re/Al$_2$O$_3$ catalyst (1 g) in the reaction medium was insufficient in order to stabilize the rapidly derived intermediates, so that they underwent thermal condensation to repolymerize into char residues. The high rate of condensation at the beginning of the reaction was confirmed by carrying out another experiment with similar amounts of Re/Al$_2$O$_3$ (1 g) and NaOH (1 g) for a total reaction time of 20 min; the yield of char generated in the first 20 min was 40.9 wt% which is 92 % of the char produced in the 6 h reaction experiment. As expected, an increase of the Re/Al$_2$O$_3$-to-NaOH ratio, by using 2 g Re/Al$_2$O$_3$ and 1 g NaOH led to a lower char yield of 23.1 wt% and, in turn, an increased monocyclic product yield of 20.9 wt%. This was further improved by a higher Re/Al$_2$O$_3$-to-NaOH ratio, and the combination of 2 g Re/Al$_2$O$_3$ and 0.5 g NaOH exhibited an even better catalytic performance, giving a high monocyclic product yield of 24.6 wt% (monocyclic saturated and aromatic hydrocarbon yields of 13.5 and 11.1 wt%, respectively) and a low char yield of 11.3 wt%. To examine whether this improvement was caused by a well-optimized Re/Al$_2$O$_3$-to-NaOH ratio or the use of an increased amount of Re/Al$_2$O$_3$, another experiment was performed using 2 g Re/Al$_2$O$_3$ with no addition of NaOH. This resulted in a monocyclic product yield of 18.6 wt% which was slightly higher than that obtained over 1 g Re/Al$_2$O$_3$ (17.5 wt%) and considerably lower than that of a catalytic system including 2 g Re/Al$_2$O$_3$ and 0.5 g NaOH (24.6 wt%), indicating that the optimum Re/Al$_2$O$_3$-to-NaOH ratio was the main reason to achieve a high monomer production. However, the char formation increased from 5.4 to 11.3 wt% when adding 0.5 g NaOH. The significance of the stabilizing effect of Re/Al$_2$O$_3$ could also be realized by the high char yield of 47.0 wt% obtained in a NaOH-catalyzed depolymerization of lignin in the absence of Re/Al$_2$O$_3$ (entry 11, Table 1).

A comparison of the yields of monocyclic products and char residues

obtained using NaOH, Re/Al$_2$O$_3$ and the combination of NaOH and Re/Al$_2$O$_3$ illustrates that the highest lignin conversion efficiency could be achieved in the presence of both NaOH and Re/Al$_2$O$_3$ (at optimum amounts). NaOH results in a high depolymerization of lignin to the intermediates which undergo condensation in the absence of Re/Al$_2$O$_3$, leading to a low yield of monocyclic products (4.2 wt%) (entry 11, Table 1). A higher monocyclic product yield of 18.6 wt% was obtained over Re/Al$_2$O$_3$ since this catalyst could effectively stabilize lignin fragments and suppress char-forming reactions (entry 12, Table 1). However, the highest monocyclic product yield of 24.6 wt% was achieved using a combination of NaOH and Re/Al$_2$O$_3$ due to the high depolymerization rate of lignin via base-catalyzed degradation on one hand, and the efficient stabilization of lignin-depolymerized fragments (suppression of condensation reactions) over Re/Al$_2$O$_3$ on the other hand (entry 10, Table 1). It could also be inferred from the results obtained at different Re/Al$_2$O$_3$-to-NaOH ratios that the correlation between the rate of lignin degradation and the rate of stabilization of lignin-depolymerized fragments is a key factor for suppressing char formation in a lignin liquefaction process. The rates of lignin depolymerization and subsequent stabilization of lignin derivatives should be well balanced to ensure that lignin derivatives can be stabilized by the applied catalytic system before they undergo repolymerization to form a large amount of char.

It is also noteworthy that no phenolics were detected in the liquid product using the combination of 2 g Re/Al$_2$O$_3$ and 0.5 g NaOH, indicating the complete HDO of phenolic compounds to hydrocarbons. Using this catalytic system, complete conversion of lignin was observed, and monocyclic saturated hydrocarbons, monocyclic aromatic hydrocarbons, tetralins, indenes and naphthalenes were the main GC-detectable organic products with the yields of 13.5, 11.1, 2.1, 1.7 and 1.2 wt%, respectively (shown in Table 3). Meanwhile, the monocyclic hydrocarbon distribution presented in Fig. 7 show that methyl-cyclohexane (16.5 wt%), (1-methylethyl)cyclohexane (7.9 wt%) and 1-ethyl-2-methylcyclohexane (7.1 wt%) were the most dominant monocyclic saturated hydrocarbons, and 1-ethyl-4-methylbenzene (6.9 wt%), ethylbenzene (5.7 wt%) and toluene (4.4 wt%) were the major monocyclic aromatic hydrocarbons. The monocyclic hydrocarbon products were composed of 23.8 wt% C$_7$-C$_9$ arenes, 21.4 wt% C$_{10}$-C$_{14}$ arenes, 46.5 wt% C$_6$-C$_9$ cycloalkanes and 8.3 wt% C$_{10}$-C$_{13}$ cycloalkanes. All GC-detectable liquid products are listed in Table S3. The molecular weight distribution of the liquid products is also shown in Fig. S7.

Scheme 1 presents a proposed network of the major series and parallel reaction pathways taking place in the catalytic liquefaction and hydrodeoxygenation of kraft lignin. First, lignin polymer is fragmented into lower weight oligomers by cleavage of C—C and C—O—C linkages through thermal cracking and NaOH-catalyzed degradation. These smaller lignin fragments can diffuse into the channels of the solid hydrotreating catalyst (e.g., ReS$_2$/Al$_2$O$_3$) and be converted into monocyclic phenolics via hydrogenolysis. Monocyclic phenolics can undergo either direct deoxygenation or ring hydrogenation to produce

monocyclic aromatic or saturated hydrocarbons, respectively. The HDO reaction selectivity could be controlled by several parameters including solvent type (polar or non-polar; solvent polarity affects solvent-reactant interactions and, in turn, the orientation of reactant adsorption on the catalyst surface), catalyst properties (oxophilicity, catalytic performance of hydrogenation active sites, hydrogen dissociation efficiency and catalyst channel size), reaction temperature (affecting hydrogenation activity and hydrogen availability on the surface of catalyst) and reaction time. In the case where free radicals of oligomers and phenolic derivatives are not well stabilized by hydrogenation, irreversible radical coupling reactions lead to rapid condensation which forms solid char residues. Therefore, the high-yield production of monocyclic hydrocarbons from the conversion of kraft lignin, using the catalytic combination of NaOH and ReS$_2$/Al$_2$O$_3$, occurs through four major steps: (i) depolymerization of lignin to oligomers via thermal cracking and alkali-catalyzed degradation; (ii) hydrogenolysis of oligomers to monocyclic phenolics over ReS$_2$/Al$_2$O$_3$; (iii) stabilization of the free radicals intermediates by ReS$_2$-catalyzed hydrogenation; (iv) hydrodeoxygenation of monocyclic phenolics to monocyclic hydrocarbons.

4. Conclusions

ReS$_2$/Al$_2$O$_3$ was a highly efficient catalyst for high-yield production of monocyclic hydrocarbons in the reductive liquefaction of a sulfur-containing lignin due to: (i) high stabilizing efficiency via hydrogenation of the free radicals of lignin-depolymerized fragments, resulting in significant suppression of char-forming condensation reactions; (ii) high hydrodeoxygenation activity leading to an efficient oxygen removal from lignin-derived phenolic compounds; (iii) resistance to sulfur poisoning. Compared to NiMo/Al$_2$O$_3$ as a conventional sulfide catalyst, ReS$_2$/Al$_2$O$_3$ led to a significantly lower char yield and higher monocyclic product yield; in the reductive liquefaction of kraft lignin at 340 °C, the alumina-supported nickel-molybdenum and rhenium sulfide catalysts resulted in char yields of 40.6 and 11.2 wt%, total monocyclic product yields of 4.6 and 21.5 wt%, and monocyclic hydrocarbon yields of 4.6 and 7.3 wt%, respectively. Char suppression over ReS$_2$/Al$_2$O$_3$ was also observed at an elevated temperature of 400 °C, giving a low char yield of 8.5 wt%. Moreover, it was shown that HDO activity is greatly affected by the choice of catalyst support; Al$_2$O$_3$-, ZrO$_2$- and HY-supported ReS$_2$ catalysts resulted in considerably different monocyclic hydrocarbon yields of 16.8, 11.2 and 8.5 wt%, respectively. This could be ascribed to different rates of dehydration and hydrogenation reactions which are affected by the acid property of the support and the sulfidation degree of the supported phase, respectively. Oxophilicity, sufficient acidity, metal-like behavior of rhenium sulfide and high dispersion of the supported phase are the significant characteristics of ReS$_2$/Al$_2$O$_3$, making this catalyst highly effective for reductive conversion of lignin into monocyclic hydrocarbons. The alkali-assisted depolymerization of lignin by an addition of NaOH clearly illustrated the significance of ReS$_2$/Al$_2$O$_3$-to-NaOH ratio which needs to be well optimized for a positive effect of NaOH addition. Otherwise, the addition of a depolymerization promoter (e.g., NaOH) higher than its optimum amount leads to an insufficient stabilization of the lignin-depolymerized fragments, and in turn, shifts the reaction pathway towards a rapid condensation and high char formation. The ReS$_2$/Al$_2$O$_3$-to-NaOH ratio of 4 g/g led to a high monocyclic hydrocarbon yield of 24.6 wt% and a low char yield of 11.3 wt%.

Table 3
Yields of GC-detectable liquid products (wt% on feed) obtained by the catalytic liquefaction of kraft lignin using 2 g Re/Al$_2$O$_3$ and 0.5 g NaOH. Reaction conditions: lignin, 3 g; hexadecane, 90 ml; reaction temperature, 400 °C; H$_2$ initial pressure, 30 bar; reaction time, 6 h.

Products	Yield (wt%)
Monocyclic saturated hydrocarbons	13.5
Monocyclic aromatic hydrocarbons	11.1
Phenolics	0.0
Tetralins	2.1
Indenes	1.7
Naphthalenes	1.2
Other hydrocarbons	6.4
Other oxygenates	3.1
Total (GC-detectable)	39.1

CRediT authorship contribution statement

Pouya Sirous-Rezaei: Conceptualization, Methodology, Investigation, Validation, Writing - original draft. **Derek Creaser:** Writing - review & editing, Supervision. **Louise Olsson:** Writing - review & editing, Supervision, Resources, Funding acquisition.
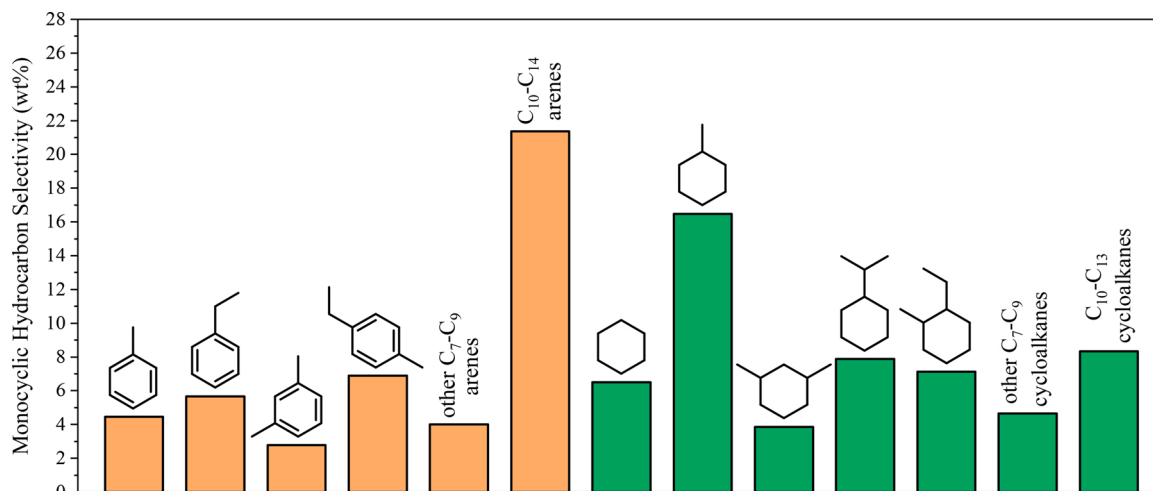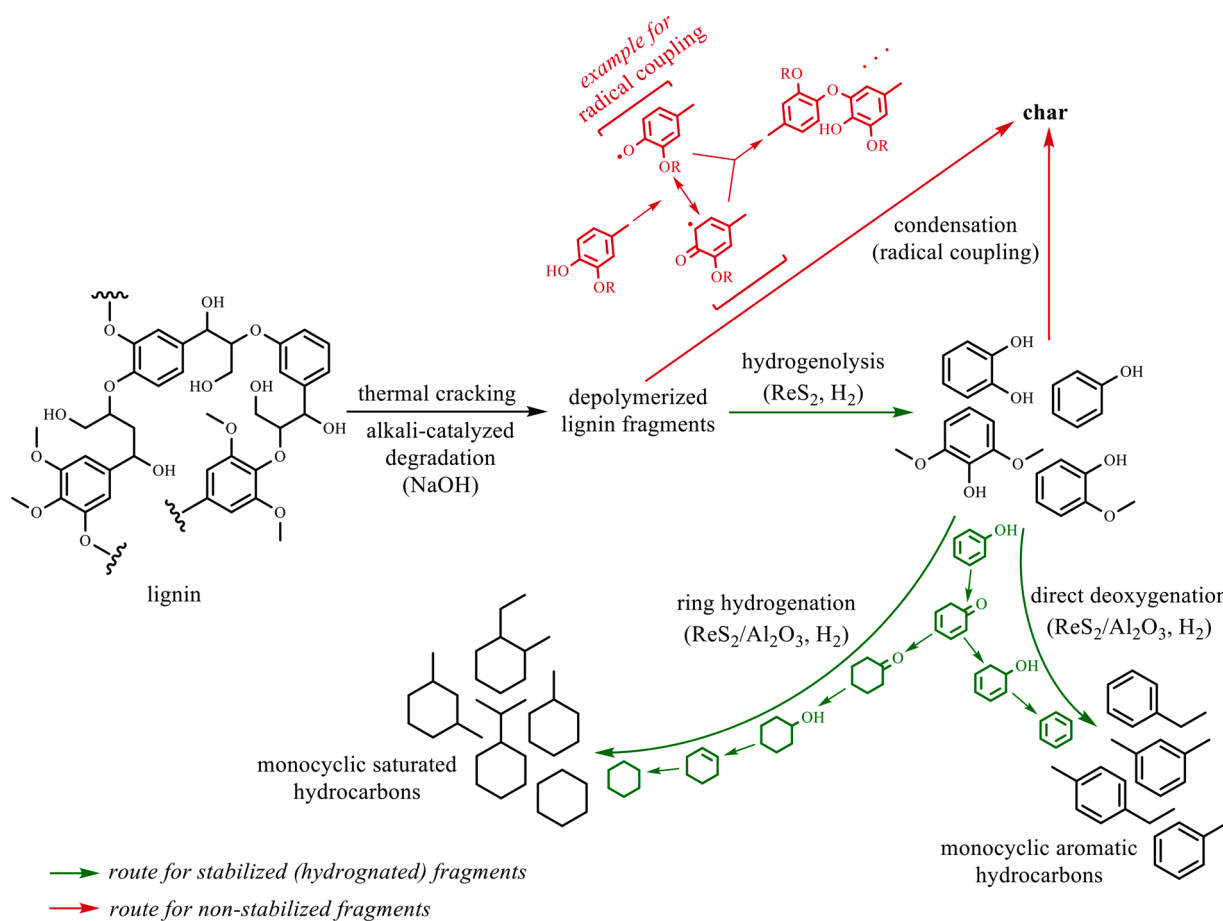
Fig. 7. Monocyclic hydrocarbon distribution (wt%) obtained by the catalytic liquefaction of kraft lignin using 2 g Re/Al$_2$O$_3$ and 0.5 g NaOH. Reaction conditions: lignin, 3 g; hexadecane, 90 ml; reaction temperature, 400 °C; H$_2$ initial pressure, 30 bar; reaction time, 6 h.

Scheme 1. Proposed reaction network for the catalytic liquefaction and hydrodeoxygenation of kraft lignin.

Declaration of Competing Interest

There are no conflicts of interest to declare.

Acknowledgements

Appendix A. Supplementary data

Supplementary material related to this article can be found, in the online version, at doi:https://doi.org/10.1016/j.apcatb.2021.120449.

References

[1] T. Ren, W. Qi, R. Su, Z. He, Promising techniques for depolymerization of lignin into value-added chemicals, ChemCatChem 11 (2019) 639–654.

[2] Z. Sun, B. Fridrich, A. de Santi, S. Elangovan, K. Barta, Bright side of lignin depolymerization: toward new platform chemicals, Chem. Rev. 118 (2018) 614–678.

[3] C. Li, X. Zhao, A. Wang, G.W. Huber, T. Zhang, Catalytic transformation of lignin for the production of chemicals and fuels, Chem. Rev. 115 (2015) 11559–11624.

[4] Q. Fang, Z. Jiang, K. Guo, X. Liu, Z. Li, G. Li, C. Hu, Low temperature catalytic conversion of oligomers derived from lignin in pubescens on Pd/NbOPO₄, Appl. Catal. B 263 (2020), 118325.

[5] L. Li, L. Dong, X. Liu, Y. Guo, Y. Wang, Selective production of ethylbenzene from lignin oil over FeOₓ modified Ru/Nb₂O₅ catalyst, Appl. Catal. B 260 (2020), 118143.

[6] V.B. Custodis, P. Hemberger, Z. Ma, J.A. van Bokhoven, Mechanism of fast pyrolysis of lignin: studying model compounds, J. Phys. Chem. B 118 (2014) 8524–8531.

[7] W. Jin, D. Shen, Q. Liu, R. Xiao, Evaluation of the co-pyrolysis of lignin with plastic polymers by TG-FTIR and Py-GC/MS, Polym. Degrad. Stab. 133 (2016) 65–74.

[8] Y. Xue, S. Zhou, X. Bai, Role of hydrogen transfer during catalytic copyrolysis of lignin and Tetralin over HZSM-5 and HY zeolite catalysts, ACS Sustain. Chem. Eng. 4 (2016) 4237–4250.

[9] M. Norgren, H. Edlund, Lignin: Recent advances and emerging applications, Curr. Opin. Colloid Interface Sci. 19 (2014) 409–416.

[10] J. Zakzeski, P.C.A. Bruijnincx, A.L. Jongerius, B.M. Weckhuysen, The catalytic valorization of lignin for the production of renewable chemicals, Chem. Rev. 110 (2010) 3552–3599.

[11] P.S. Rezaei, H. Shafaghat, W.M.A.W. Daud, Production of green aromatics and olefins by catalytic cracking of oxygenate compounds derived from biomass pyrolysis: a review, Appl. Catal. A 469 (2014) 490–511.

[12] X. Li, L. Su, Y. Wang, Y. Yu, C. Wang, X. Li, Z. Wang, Catalytic fast pyrolysis of Kraft lignin with HZSM-5 zeolite for producing aromatic hydrocarbons, Front. Environ. Sci. Eng. 6 (2012) 295–303.

[13] M.P. Pandey, C.S. Kim, Lignin depolymerization and conversion: a review of thermochemical methods, Chem. Eng. Technol. 34 (2011) 29–41.

[14] J. Pu, T.-S. Nguyen, E. Leclerc, C. Lorentz, D. Laurenti, I. Pitault, M. Tayakout-Fayolle, C. Geantet, Lignin catalytic hydroconversion in a semi-continuous reactor: an experimental study, Appl. Catal. B 256 (2019), 117769.

[15] X. Dou, W. Li, C. Zhu, X. Jiang, Catalytic waste Kraft lignin hydrodeoxygenation to liquid fuels over a hollow Ni-Fe catalyst, Appl. Catal. B 287 (2021), 119975.

[16] X. Dou, X. Jiang, W. Li, C. Zhu, Q. Liu, Q. Lu, X. Zheng, H.-m. Chang, H. Jameel, Highly efficient conversion of Kraft lignin into liquid fuels with a Co-Zn-beta zeolite catalyst, Appl. Catal. B 268 (2020), 118429.

[17] W. Schutyser, T. Renders, S. Van den Bosch, S.F. Koelewijn, G.T. Beckham, B. F. Sels, Chemicals from lignin: an interplay of lignocellulose fractionation, depolymerisation, and upgrading, Chem. Soc. Rev. 47 (2018) 852–908.

[18] P.J. Deuss, K. Barta, From models to lignin: transition metal catalysis for selective bond cleavage reactions, Coord. Chem. Rev. 306 (2016) 510–532.

[19] H. Wang, H. Ben, H. Ruan, L. Zhang, Y. Pu, M. Feng, A.J. Ragauskas, B. Yang, Effects of lignin structure on hydrodeoxygenation reactivity of pine wood lignin to valuable chemicals, ACS Sustain. Chem. Eng. 5 (2017) 1824–1830.

[20] J. Hu, D. Shen, S. Wu, H. Zhang, R. Xiao, Effect of temperature on structure evolution in char from hydrothermal degradation of lignin, J. Anal. Appl. Pyrolysis 106 (2014) 118–124.

[21] C. Zhang, Y. Shao, L. Zhang, S. Zhang, R.J.M. Westerhof, Q. Liu, P. Jia, Q. Li, Y. Wang, X. Hu, Impacts of temperature on evolution of char structure during pyrolysis of lignin, Sci. Total Environ. 699 (2020) 134381.

[22] X. Huang, C. Atay, J. Zhu, S.W.L. Palstra, T.I. Koranyi, M.D. Boot, E.J.M. Hensen, Catalytic depolymerization of lignin and woody biomass in supercritical ethanol: influence of reaction temperature and feedstock, ACS Sustain. Chem. Eng. 5 (2017) 10864–10874.

[23] P.S. Rezaei, H. Shafaghat, W.M.A.W. Daud, Aromatic hydrocarbon production by catalytic pyrolysis of palm kernel shell waste using a bifunctional Fe/HBeta catalyst: effect of lignin-derived phenolics on zeolite deactivation, Green Chem. 18 (2016) 1684–1693.

[24] P. Sirous-Rezaei, Y.-K. Park, Catalytic hydropyrolysis of lignin: suppression of coke formation in mild hydrodeoxygenation of lignin-derived phenolics, Chem. Eng. J. 386 (2020), 121348.

[25] T. Nakamura, H. Kawamoto, S. Saka, Condensation reactions of some lignin related compounds at relatively low pyrolysis temperature, J. Wood Chem. Technol. 27 (2007) 121–133.

[26] S. Kasakov, H. Shi, D.M. Camaioni, C. Zhao, E. Baráth, A. Jentys, J.A. Lercher, Reductive deconstruction of organosolv lignin catalyzed by zeolite supported nickel nanoparticles, Green Chem. 17 (2015) 5079–5090.

[27] H. Wang, H. Ruan, H. Pei, H. Wang, X. Chen, M.P. Tucker, J.R. Cort, B. Yang, Biomass-derived lignin to jet fuel range hydrocarbons via aqueous phase hydrodeoxygenation, Green Chem. 17 (2015) 5131–5135.

[28] K. Barta, G.R. Warner, E.S. Beach, P.T. Anastas, Depolymerization of organosolv lignin to aromatic compounds over Cu-doped porous metal oxides, Green Chem. 16 (2014) 191–196.

[29] Y. Shao, Q. Xia, L. Dong, X. Liu, X. Han, S.F. Parker, Y. Cheng, L.L. Daemen, A. J. Ramirez-Cuesta, S. Yang, Y. Wang, Selective production of arenes via direct lignin upgrading over a niobium-based catalyst, Nat. Commun. 8 (2017), 16104.

[30] J. Kong, M. He, J.A. Lercher, C. Zhao, Direct production of naphthenes and paraffins from lignin, Chem. Commun. 51 (2015) 17580–17583.

[31] S. Agarwal, R.K. Chowdari, I. Hita, H.J. Heeres, Experimental studies on the hydrotreatment of kraft lignin to aromatics and alkylphenolics using economically viable Fe-Based catalysts, ACS Sustain. Chem. Eng. 5 (2017) 2668–2678.

[32] C.R. Kumar, N. Anand, A. Kloekhorst, C. Cannilla, G. Bonura, F. Frusteri, K. Barta, H.J. Heeres, Solvent free depolymerization of Kraft lignin to alkyl-phenolics using supported NiMo and CoMo catalysts, Green Chem. 17 (2015) 4921–4930.

[33] A. Kloekhorst, H.J. Heeres, Catalytic hydrotreatment of alcell lignin using supported Ru, Pd, and Cu catalysts, ACS Sustain. Chem. Eng. 3 (2015) 1905–1914.

[34] I. Hita, P.J. Deuss, G. Bonura, F. Frusteri, H.J. Heeres, Biobased chemicals from the catalytic depolymerization of Kraft lignin using supported noble metal-based catalysts, Fuel Process. Technol. 179 (2018) 143–153.

[35] B. Zhang, Z. Qi, X. Li, J. Ji, L. Zhang, H. Wang, X. Liu, C. Li, Cleavage of lignin C-O bonds over a heterogeneous rhenium catalyst through hydrogen transfer reactions, Green Chem. 21 (2019) 5556–5564.

[36] L.-P. Xiao, S. Wang, H. Li, Z. Li, Z.-J. Shi, L. Xiao, R.-C. Sun, Y. Fang, G. Song, Catalytic hydrogenolysis of lignins into phenolic compounds over carbon nanotube supported molybdenum oxide, ACS Catal. 7 (2017) 7535–7542.

[37] S. Guadix-Montero, M. Sankar, Review on catalytic cleavage of C-C inter-unit linkages in lignin model compounds: towards lignin depolymerisation, Top. Catal. 61 (2018) 183–198.

[38] N. Escalona, M. Vrinat, D. Laurenti, F.J. Gil Llambías, Rhenium sulfide in hydrotreating, Appl. Catal. A 322 (2007) 113–120.

[39] K. Tomishige, Y. Nakagawa, M. Tamura, Taming heterogeneous rhenium catalysis for the production of biomass-derived chemicals, Chin. Chem. Lett. 31 (2020) 1071–1077.

[40] C. Alvarez, K. Cruces, R. Garcia, C. Sepulveda, J.L.G. Fierro, I.T. Ghampson, N. Escalona, Conversion of guaiacol over different Re active phases supported on CeO₂-Al₂O₃, Appl. Catal. A 547 (2017) 256–264.

[41] K. Leiva, N. Martinez, C. Sepulveda, R. García, C.A. Jiménez, D. Laurenti, M. Vrinat, C. Geantet, J.L.G. Fierro, I.T. Ghampson, N. Escalona, Hydrodeoxygenation of 2-methoxyphenol over different Re active phases supported on SiO₂ catalysts, Appl. Catal. A 490 (2015) 71–79.

[42] C. Sepúlveda, R. García, P. Reyes, I.T. Ghampson, J.L.G. Fierro, D. Laurenti, M. Vrinat, N. Escalona, Hydrodeoxygenation of guaiacol over ReS₂/activated carbon catalysts. Support and Re loading effect, Appl. Catal., A 475 (2014) 427–437.

[43] X. Zhu, L.L. Lobban, R.G. Mallinson, D.E. Resasco, Bifunctional transalkylation and hydrodeoxygenation of anisole over a Pt/HBeta catalyst, J. Catal. 281 (2011) 21–29.

[44] F.E. Massoth, P. Politzer, M.C. Concha, J.S. Murray, J. Jakowski, J. Simons, Catalytic hydrodeoxygenation of methyl-substituted phenols: correlations of kinetic parameters with molecular properties, J. Phys. Chem. B 110 (2006) 14283–14291.

[45] P. Sirous-Rezaei, J. Jae, J.-M. Ha, C.H. Ko, J.M. Kim, J.-K. Jeon, Y.-K. Park, Mild hydrodeoxygenation of phenolic lignin model compounds over a FeReOₓ/ZrO₂ catalyst: zirconia and rhenium oxide as efficient dehydration promoters, Green Chem. 20 (2018) 1472–1483.

[46] C. Chen, G. Chen, F. Yang, H. Wang, J. Han, Q. Ge, X. Zhu, Vapor phase hydrodeoxygenation and hydrogenation of m-cresol on silica supported Ni, Pd and Pt catalysts, Chem. Eng. Sci. 135 (2015) 145–154.

[47] Y. Romero, F. Richard, S. Brunet, Hydrodeoxygenation of 2-ethylphenol as a model compound of bio-crude over sulfided Mo-based catalysts: promoting effect and reaction mechanism, Appl. Catal. B 98 (2010) 213–223.

[48] P.T.M. Do, S. Crossley, M. Santikunaporn, D.E. Resasco, Catalytic strategies for improving specific fuel properties, Catalysis (2007) 33–64.

[49] K.H. Kim, C.S. Kim, Recent efforts to prevent undesirable reactions from fractionation to depolymerization of lignin: toward maximizing the value from lignin, Front. Energy Res. 6 (2018).

[50] C. Herrera, I.T. Ghampson, K. Cruces, C. Sepúlveda, L. Barrientos, D. Laurenti, C. Geantet, R. Serpell, D. Contreras, V. Melin, N. Escalona, Valorization of biomass derivatives through the conversion of phenol over silica-supported Mo-Re oxide catalysts, Fuel 259 (2020), 116245.

[51] K. Leiva, R. Garcia, C. Sepulveda, D. Laurenti, C. Geantet, M. Vrinat, J.L. Garcia-Fierro, N. Escalona, Conversion of guaiacol over supported ReOₓ catalysts: support and metal loading effect, Catal. Today 296 (2017) 228–238.

[52] D. Laurenti, K.T.N. Thi, N. Escalona, L. Massin, M. Vrinat, F.J.G. Llambías, Support effect with rhenium sulfide catalysts, Catal. Today 130 (2008) 50–55.

[53] N. Escalona, J. Ojeda, R. Cid, G. Alves, A. López Agudo, J.L.G. Fierro, F.J. G. Llambías, Characterization and reactivity of Re(x)/γ-Al₂O₃ catalysts in hydrodesulfurization and hydrodenitrogenation of gas oil: effect of Re loading, Appl. Catal. A 234 (2002) 45–54.

[54] J. Hu, S. Zhang, R. Xiao, X. Jiang, Y. Wang, Y. Sun, P. Lu, Catalytic transfer hydrogenolysis of lignin into monophenols over platinum-rhenium supported on titanium dioxide using isopropanol as in situ hydrogen source, Bioresour. Technol. 279 (2019) 228–233.

[55] N. Martínez, R. García, J.L.G. Fierro, C. Wheeler, R.N. Austin, J.R. Gallagher, J. T. Miller, T.R. Krause, N. Escalona, C. Sepúlveda, Effect of Cu addition as a promoter on Re/SiO₂ catalysts in the hydrodeoxygenation of 2-methoxyphenol as a model bio oil compound, Fuel 186 (2016) 112–121.

[56] X. Li, B. Zhang, X. Pan, J. Ji, Y. Ren, H. Wang, N. Ji, Q. Liu, C. Li, One-pot conversion of lignin into naphthenes catalyzed by a heterogeneous rhenium oxide-modified iridium compound, ChemSusChem 13 (2020) 4409–4419.

[57] P. Sirous-Rezaei, J. Jae, K. Cho, C.H. Ko, S.-C. Jung, Y.-K. Park, Insight into the effect of metal and support for mild hydrodeoxygenation of lignin-derived phenolics to BTX aromatics, Chem. Eng. J. 377 (2019), 120121.

[58] H.H. Ingelsten, M. Skoglundh, E. Fridell, Influence of the support acidity of Pt/aluminum-silicate catalysts on the continuous reduction of NO under lean conditions, Appl. Catal. B 41 (2003) 287–300.

[59] V. Schwartz, V.T. da Silva, S.T. Oyama, Push–pull mechanism of hydrodenitrogenation over carbide and sulfide catalysts, J. Mol. Catal. A Chem. 163 (2000) 251–268.

[60] H. Shafaghat, P.S. Rezaei, W.M. Ashri Wan Daud, Effective parameters on selective catalytic hydrodeoxygenation of phenolic compounds of pyrolysis bio-oil to high-value hydrocarbons, RSC Adv. 5 (2015) 103999–104042.

[61] B. Yoosuk, D. Tumnantong, P. Prasassarakich, Unsupported MoS_2 and $CoMoS_2$ catalysts for hydrodeoxygenation of phenol, Chem. Eng. Sci. 79 (2012) 1–7.

[62] Y. Yang, Ha. Luo, G. Tong, K.J. Smith, C.T. Tye, Hydrodeoxygenation of phenolic model compounds over MoS_2 catalysts with different structures, Chin. J. Chem. Eng. 16 (2008) 733–739.

[63] P. Sirous Rezaei, H. Shafaghat, W.M.A.W. Daud, Suppression of coke formation and enhancement of aromatic hydrocarbon production in catalytic fast pyrolysis of cellulose over different zeolites: effects of pore structure and acidity, RSC Adv. 5 (2015) 65408–65414.

[64] H. Iida, A. Igarashi, Structure characterization of Pt-Re/TiO_2 (rutile) and Pt-Re/ZrO_2 catalysts for water gas shift reaction at low-temperature, Appl. Catal. A 303 (2006) 192–198.

[65] J. Quartararo, S. Mignard, S. Kasztelan, Hydrodesulfurization and hydrogenation activities of alumina- supported transition metal sulfides, J. Catal. 192 (2000) 307–315.

[66] V.M. Roberts, V. Stein, T. Reiner, A. Lemonidou, X. Li, J.A. Lercher, Towards quantitative catalytic lignin depolymerization, Chemistry 17 (2011) 5939–5948.

[67] A. Toledano, L. Serrano, J. Labidi, Organosolv lignin depolymerization with different base catalysts, J. Chem. Technol. Biotechnol. 87 (2012) 1593–1599.